*Inorg. Chem.* **2007**, *46*, 4028–4035


# $Au_3SnP_7$@Black Phosphorus: An Easy Access to Black Phosphorus

**Stefan Lange,[†] Peer Schmidt,[‡] and Tom Nilges*[,†]**

*Institut für Anorganische und Analytische Chemie, Universität Münster, Corrensstrasse 30, D-48149 Münster, Germany, and Institut für Anorganische Chemie, Technische Universität Dresden, Helmholtzstrasse 10, D-01069 Dresden, Germany*

Received November 17, 2006

Black phosphorus can be prepared under low-pressure conditions at 873 K from red phosphorus via the addition of small quantities of gold, tin, and tin(IV) iodide. $Au_3SnP_7$, AuSn, and $Sn_4P_3$ were observed as additional phases. Tin(IV) iodide remains unreacted during the preparation process. The crystal structure of black phosphorus was redetermined from single crystals. P (295 K): $a = 3.316(1)$ Å, $b = 10.484(2)$ Å, $c = 4.379(1)$ Å, $V = 152.24(6)$ Å$^3$, space group *Cmce* (No. 64). Solid-state $^{31}$P MAS NMR spectroscopy and X-ray powder diffraction were performed to substantiate the high crystal quality of black phosphorus. A possible mechanism for the formation is discussed in terms of the comparable structural features of black phosphorus and $Au_3SnP_7$. Thermodynamic calculations showed that the only relevant gas-phase species, $P_4$, and the transport reactions are not suitable for the preparation of orthorhombic black phosphorus at temperatures above 773 K. A kinetically controlled mechanism must be favored instead of a thermodynamically controlled formation. The new preparation method of black phosphorus represents an easy and effective way to avoid complicated preparative setups, toxic catalysts, or "dirty" flux methods and is of general interest in elemental chemistry.

## Introduction

A large number of phosphorus modifications are known to date. Cubic white phosphorus[1] (e.g., $\gamma$-$P_4$), amorphous red phosphorus (hereafter abbreviated as P(red)) with various degrees of disorder, the two allotropes of red phosphorus, the violet[2,3] and fibrous phosphorus,[4] and orthorhombic black phosphorus[5] (hereafter abbreviated as P(black)) are the main ones. Recently, some theoretically predicted allotropic modifications[6] were isolated from a copper halide matrix.[7] A great diversity of physical properties, an extraordinary structural chemistry, and quite different chemical reactivity are outstanding features in the field of phosphorus chemistry.[8]

In the late nineteenth century, with the first reports on black phosphorus, great interest emerged for the determination and understanding of the physical properties of black phosphorus. Black phosphorus, known to be the modification of highest density and also the least reactive one, can be prepared using three classical routes.[9] Historically, the synthesis under high-pressure conditions from white and red phosphorus[10−12] was followed by preparation using mercury[13] and the bismuth-flux method.[14−16] Semiconducting black phosphorus (p-type) shows several pressure-induced and temperature-dependent phase transitions to a rhombohedral, semimetallic, and cubic metallic phase.[17,18] Black phosphorus crystallizes orthorhombically at standard conditions and

* To whom correspondence should be addressed. Phone: +49-251-83-36645. Fax: +49-251-83-36002. E-mail: nilges@uni-muenster.de.
[†] Universität Münster.
[‡] Technische Universität Dresden.

(1) Okudera, H.; Dinnebier, R. E.; Simon, A. *Z. Kristallogr.* **2005**, *220*, 259−264.
(2) Hittorf, W. *Ann. Phys. Chem.* **1865**, *126*, 193−215.
(3) Thurn, H.; Krebs, H. *Acta Crystallogr., Sect. B* **1969**, *25*, 125−135.
(4) Ruck, M.; Hoppe, D.; Wahl, B.; Simon, P.; Wang, Y.; Seifert, G. *Angew. Chem.* **2005**, *117*, 7788−7792; *Angew. Chem., Int. Ed.* **2005**, *44*, 7616−7619.
(5) Hultgren, R.; Gingrich, N. S.; Warren, B. E. *J. Chem. Phys.* **1935**, *3*, 351−355.
(6) Böcker, S.; Häser, M. *Z. Anorg. Allg. Chem.* **1995**, *621*, 258−286.
(7) Pfitzner, A.; Bräu, M. F.; Zweck, J.; Brunklaus, G.; Eckert, H. *Angew. Chem.* **2004**, 4324−4327; *Angew. Chem., Int. Ed.* **2004**, *43*, 4228−4231.
(8) Pfitzner, A. *Angew. Chem.* **2006**, *118*, 714−715; *Angew. Chem., Int. Ed.* **2006**, *45*, 699−700.
(9) Chang, K. J.; Cohen, M. L. *Phys. Rev. B* **1986**, 6177−6186.
(10) Bridgman, P. W. *J. Am. Chem. Soc.* **1914**, *36*, 1344−1363.
(11) Bridgman, P. W. *Phys. Rev.* **1914**, *3*, 153−203.
(12) Bridgman, P. W. *Proc. Am. Acad. Arts Sci.* **1948**, *76*, 55−70.
(13) Krebs, H.; Weitz, H.; Worms, K. H. *Z. Anorg. Allg. Chem.* **1955**, *280*, 119−133.
(14) Brown, A.; Rundquist, S. *Acta Crystallogr.* **1965**, *19*, 684−685.
(15) Maruyama, Y.; Suzuki, S.; Kobayashi, K.; Tanuma, S. *Phys. B−C* **1981**, *105*, 99−102.
(16) Baba, M.; Izumida, F.; Takeda, Y.; Morita, A. *Jpn. J. Appl. Phys.* **1989**, *28*, 1019−1022.
(17) Jamieson, J. C. *Science* **1963**, *139*, 1291−1292.
(18) Morita, A. *Appl. Phys. A* **1986**, *39*, 227−242 and references therein.



10.1021/ic062192q CCC: $37.00 
Published on Web 04/18/2007

consists of puckered layers orientated parallel to the *ac* plane.[14]

Until the late 1970s, the lack of big and high-quality crystals slowed the investigation of interesting properties such as polymorphic phase transitions, electric conductivity, and pressure-dependent superconductivity.[18] This problem was solved by the preparation of large ($4 \times 2 \times 0.2$ to $5 \times 5 \times 10$ $mm^3$) crystals using wedge-type[19] and multianvil-type[20] apparatus at pressures between 3.8 and 1 GPa. Very recently black phosphorus was drawn back into the focus of material scientists as an anode material for lithium ion batteries.[21] A simple, nontoxic, and effective preparation method is necessary for a successful application for industrial production. The classical preparation methods stated above do not fulfill all of these aspects. The uses of noncatalytic amounts of mercury or melt-syntheses like the bismuth-flux method are either toxic or time-consuming in the workup procedures. An interesting but rather complicated and operatively expensive method was reported by Baillargeon et al. to make black phosphorus from red phosphorus by thermal cycling in a three-step process in an ultrahigh vacuum ($p = 10^{-8}$ Torr) using tantalum and BN containers.[22] After almost 100 years of scientific research, it is still a challenge to prepare black phosphorus in an appropriate way for industrial applications.

Phosphorus, in various modifications, can be easily transferred to a plethora of phosphides by reacting with almost every element of the periodic table. The extraordinary structural and chemical variability of phosphorus defines the huge field of phosphide and polyphosphide solid-state chemistry.[23,24]

On our way to prepare new polyphosphides, we focused on solid-state reactions with mineralizing agents as reaction promoters.[25] Following this concept, we succeeded in the preparation of $M_3SnCuP_{10}$ containing $Ag_3Sn$ and $Au_3Sn$ heteroclusters and adamantane analogue $P_{10}$ cages.[26,27] Heteroclusters like $Cu_3Sn$ in $Cu_4SnP_{10}$[28,29] and $Ag_3Sn$ or $Au_3Sn$ in $M_3SnP_7$[27,30] are the only examples of $M_3M'$ clusters stabilized in a polyphosphide substructure.

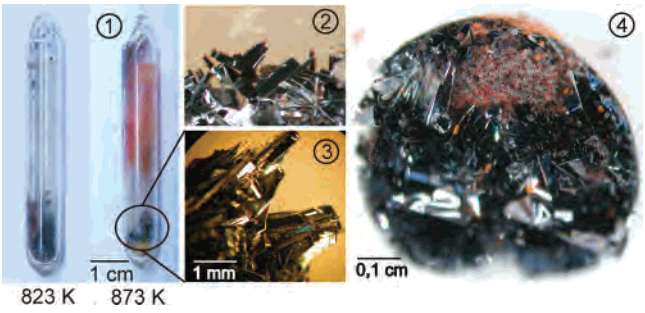


**Figure 1.** Silica ampules (picture 1) used for the preparation of **1** (picture 3). Sn(IV) iodide condensed on top of **1** after thermal decomposition of **2** at 1073 K (picture 2). Representative batch of black phosphorus grown on top of a $Au_3SnP_7$/AuSn bulk (picture 4). The mineralization agent $SnI_4$ (orange dots) is well separated from the bulk materials and **1** (pictures 2 and 4).

This preparative clue also led to a success in the preparation of P(black).

## Experimental Section

**Preparation.** $SnI_4$ was prepared by mixing tin (12 g, 0.10 mol) and iodine (40 g, 0.16 mol) in toluene (250 mL).[31] The mixture was refluxed for ~30 min until the violet color of the iodine disappeared. The hot solution was decanted from the remaining tin. Orange $SnI_4$ crystallized after the mixture was cooled to room temperature. The crude product was recrystallized from toluene and dried over molecular sieves.

Black phosphorus (**1**) was prepared by the reaction of gold (70.5 mg, 0.358 mmole, 99.9%, foil, Chempur), tin (42.5 mg, 0.358 mmole, 99.999%, ingots, Heraeus), red phosphorus (155.2 mg, 5.011 mmole, 99.999+ %, pieces, Chempur), and $SnI_4$ (10.0 mg, 0.016 mmole, recrystallized) in evacuated ($p = 10^{-3}$ mbar) silica ampules (length 50 mm, inner diameter 8 mm). The starting materials were heated to 823, 873, or 923 K and kept at this temperature for 5−10 days. Compound **1**, grown on top of the bulk material (see Figure 1) consisting of either $Au_3SnP_7$ (**2**) and $Sn_4P_3$ (**3**) (873 K) or of $Au_3SnP_7$ (**2**) and AuSn (**4**) (923 K), can be separated mechanically.

The remaining reaction promoter $SnI_4$ was dissolved in hot toluene. Different preparation routes have been tried to optimize the reaction procedure and to analyze the role of the reaction promoter and the binary and ternary phosphides (Table 1).

**X-ray Powder Diffraction.** Phase analytical measurements were performed using a Stoe StadiP powder diffractometer or Guinier cameras operated with Cu $K\alpha_1$ radiation ($\lambda = 1.5406$ Å). Both machines were fitted with a linear 5° PSD (Braun) in case of the StadiP diffractometer or image plate technology (Guinier) as detection units. Data were collected in the $2\theta$ range of 10−100° with silicon (StadiP) and α-quartz (Guinier) as external and internal standards. Data readout of the image plates was done using a BAS 1800 reader (Fuji), and the WinXpow program package was used for indexing and refinement purposes.[32]

**Single-Crystal X-ray Diffraction.** Intensity data of suitable phosphorus single crystals were collected on a IPDS II at 293 K operated with Mo Kα radiation ($\lambda = 0.71073$ Å). A numerical absorption correction was applied to the data after optimization of the crystal shape from symmetry equivalent reflections.[33]

(19) Shirotani, I.; Maniwa, R.; Sato, H.; Fukizawa, A.; Sato, N.; Maruyama, Y.; Kajiwara, T.; Inokuchi, H.; Akimoto, S. *Nippon Kagaku Kaishi* **1981**, *10*, 1604−1609.
(20) Endo, S.; Akahama, Y.; Terada, S.; Narita, S. *J. Appl. Phys.* **1982**, *21*, L482−L484.
(21) Qi, L.; Hu, X.; Chen, H.; Mao, Y. Faming Zhuanli Shenqing Gongkai Shuomingshu. Patent CN 1481040, 2004, 6 pp.
(22) Baillargeon, J. N.; Cheng, K.-Y.; Cho, A. Y.; Chu, S.-N. G.; Hwang, W.-Y. US Patent 6110438, 2000.
(23) Hönle, W.; von Schnering, H. G. *Z. Kristallogr.* **1980**, *153*, 339−350.
(24) Pöttgen, R.; Hönle, W.; von Schnering, H. G. in *Encyclopedia of Inorganic Chemistry*, 2nd ed.; King, R. B., Ed.; Wiley: Chichester, U.K., 2005; Vol. VIII, pp 4255−4308.
(25) Lange, S.; Sebastian, C. P.; Nilges, T. *Z. Anorg. Allg. Chem.* **2006**, *632*, 195−203.
(26) Lange, S.; Sebastian, C. P.; Zhang, L.; Eckert, H.; Nilges, T. *Inorg. Chem.* **2006**, *45*, 5878−5885.
(27) Lange, S.; Nilges, T. *Z. Naturforsch.* **2006**, *61b*, 871−881.
(28) Goryunova, N. A.; Orlov, V. M.; Sokolova, V. I.; Shepenkov, G. P.; Tsvetkova, E. V. *Phys. Status Solidi A* **1970**, *3*, 75−87.
(29) von Schnering, H. G.; Hönle, W. *Chem. Rev.* **1988**, *88*, 243−273.
(30) Shatruk, M. M.; Kovnir, K. A.; Shevelkov, A. V.; Popovkin, B. A. *Angew. Chem.* **2000**, *112*, 2561−2562; *Angew. Chem., Int. Ed.* **2000**, *39*, 2508−2509.
(31) Brauer, G. *Handbuch der Präparativen Anorganischen Chemie*, 3rd ed.; F. Enke: Stuttgart, Germany, 1978; Vol. 2, p 759.
(32) *WinXpow*, version 1.25; Stoe & Cie GmbH: Darmstadt, Germany, 2004.

**Electron Microscopy.** Semiquantitative elementary analysis was performed with a Leica 420i scanning electron microscope (Zeiss) fitted with an electron-dispersive detector unit (Oxford) and Au, Sn, and GaP as standards for calibration. A voltage of 20 kV was applied to the samples.

**$^{31}$P MAS NMR Spectroscopy.** Solid-state $^{31}$P NMR spectra were recorded at resonance frequencies of 202.5 MHz on a Bruker DSX-500 spectrometer, using a 2.5 mm probe at a magic angle spinning (MAS) frequency of 25 kHz. The acquisition parameters were a pulse length of 3.0 $\mu$s (90°) and a recycle delay of 150 s. A total of 160 scans was accumulated. The chemical shift is referenced to 85% $H_3PO_4$.

**Thermodynamic Calculations.** The estimation of unknown thermodynamic data in general and the determination of the data for the present calculations will be shown for $\mathbf{2}_{(s)}$. The formation of $\mathbf{2}_{(s)}$ in the ternary system Au/Sn/P can be described formally by the following solid-state equilibria 1−5

$$Au_2P_{3(s)} + AuSn_{(s)} + 4P_{(s,red)} = Au_3SnP_{7(s)} \quad (1)$$

$$^5/_4Au_2P_{3(s)} + {}^2/_4AuSn_{2(s)} + {}^{13}/_4P_{(s,red)} = Au_3SnP_{7(s)} \quad (2)$$

$$^{11}/_8Au_2P_{3(s)} + {}^2/_8AuSn_{4(s)} + {}^{23}/_8P_{(s,red)} = Au_3SnP_{7(s)} \quad (3)$$

$$^6/_4Au_2P_{3(s)} + {}^1/_4Sn_4P_{3(s)} + {}^7/_4P_{(s,red)} = Au_3SnP_{7(s)} \quad (4)$$

$$^9/_6Au_2P_{3(s)} + {}^2/_6Sn_3P_{4(s)} + {}^7/_6P_{(s,red)} = Au_3SnP_{7(s)} \quad (5)$$

Assuming that $(\mathbf{2})_{(s)}$ exists under thermodynamically equilibrated conditions, $\Delta G^\circ_R < 0$ is valid for reactions 1−5. The reaction entropies can be estimated from the NEUMANN−KOPP rules for solid-state reactions to $\Delta S^\circ_R \approx 0$ ($S^\circ(Au_3SnP_{7(s)}) = \sum[v_iS^\circ(i)]$). From $\Delta G^\circ_R < 0$, one can conclude $\Delta H^\circ_R < 0$, which leads to the standard enthalpy of formation $\Delta H^\circ_B(Au_3SnP_{7(s)}) < \sum[v_i\Delta H^\circ_B(i)]$ ($i$ = $Au_2P_3$, AuSn, $AuSn_2$, $AuSn_4$, $Sn_4P_3$, $Sn_3P_4$).

Using the reaction data

$$\sum[v_i\Delta H^\circ_B(i)]_{(1)} = -200 \text{ kJ mol}^{-1}$$
$$\sum[v_iS^\circ(i)]_{(1)} = 338 \text{ J mol}^{-1}\text{ K}^{-1}$$
$$\sum[v_i\Delta H^\circ_B(i)]_{(2)} = -203 \text{ kJ mol}^{-1}$$
$$\sum[v_iS^\circ(i)]_{(2)} = 332 \text{ J mol}^{-1}\text{ K}^{-1}$$
$$\sum[v_i\Delta H^\circ_B(i)]_{(3)} = -197 \text{ kJ mol}^{-1}$$
$$\sum[v_iS^\circ(i)]_{(3)} = 333 \text{ J mol}^{-1}\text{ K}^{-1}$$
$$\sum[v_i\Delta H^\circ_B(i)]_{(4)} = -213 \text{ kJ mol}^{-1}$$
$$\sum[v_iS^\circ(i)]_{(4)} = 325 \text{ J mol}^{-1}\text{ K}^{-1}$$
$$\sum[v_i\Delta H^\circ_B(i)]_{(5)} = -214 \text{ kJ mol}^{-1}$$
$$\sum[v_iS^\circ(i)]_{(5)} = 331 \text{ J mol}^{-1}\text{ K}^{-1}$$

one can directly derive the standard data for **2**

$$\Delta H^\circ_B(Au_3SnP_{7(s),298}) = -250(10) \text{ kJ mol}^{-1}$$
$$S^\circ(Au_3SnP_{7(s),298}) = 332(5) \text{ J mol}^{-1}\text{ K}^{-1}$$

(33) (a) *X-RED 32*, version 1.10; Stoe & Cie GmbH: Darmstadt, Germany, 2004. (b) *X-SHAPE*, version 2.05; Stoe & Cie GmbH: Darmstadt, Germany, 2004.

**Table 1.** Thermodynamic Data of the Solid Phases in the Au/Sn/P System.

| compound | $\Delta H^\circ_{B298}$ (kJ mol$^{-1}$) | $S^\circ_{B298}$ (J mol$^{-1}$ K$^{-1}$) | $C_p/a$ (J mol$^{-1}$ K$^{-1}$) | $b \times 10^{-3}$ $T$ | $c \times 10^6$ $T^{-2}$ | ref |
|---|---|---|---|---|---|---|
| Au | 0.0 | 47.5 | 31.5 | −13.5 | −0.3 | 36 |
| $Sn_{(s)}$ | 0.0 | 51.2 | 21.6 | 18.2 | 0.0 | 36 |
| $Sn_{(l)}$ | 6.8 | 64.5 | 21.7 | 6.1 | 1.3 | 36 |
| P(red) | −17.5 | 22.8 | 16.7 | 14.9 | 0.0 | 36 |
| $Au_2P_3$ | −99.5 | 149.1 | 108.4 | 37.7 | 0.0 | 36 |
| AuSn | −30.5 | 98.1 | 46.6 | 15.9 | 0.0 | 37 |
| $AuSn_2$ | −42.4 | 135.6 | 83.9 | 19.7 | 0.0 | 37 |
| | | 142.3 | | | | *a* |
| $AuSn_4$ | −38.7 | 250.6 | 137.9 | 33.1 | 0.0 | 37 |
| | −41.2 | | | | | *a* |
| $Sn_4P_3$ | −138.0 | 231.0 | 151.0 | 78.6 | 0.0 | *a* |
| $Sn_3P_4$ | −131.0 | 225.0 | 151.0 | 62.4 | 0.0 | *a* |
| $Au_3SnP_7$ | −250.0 | 332.0 | 145.6 | 64.5 | 0.0 | *a* |

[a] Optimized value, this work

Those values were used for model calculations to derive a consistent description of the experimentally observed phases in the system Au/Sn/P. All thermodynamic data used are summarized in Table 1.

Chemical transport phenomena and reactions were calculated using the extended transport model reported by Krabbes et al., implemented in the program package TRAGMIN 4.01.[34,35]

## Results and Discussion

**Preparation of Black Phosphorus: Preparative Aspects.** Black phosphorus (**1**) in high yield, based on the amount of the starting material red phosphorus, can be obtained from a mixture of red P, Au, Sn, $SnI_4$ reacting in evacuated ($p_{min}$ of approximately $10^{-3}$ mbar) silica ampules at 823, 873, or 923 K. X-ray powder diffraction phase analysis pointed toward some additional crystalline products formed by the reaction of Au, Sn, and red phosphorus after the annealing process at 823 and 873 or 923 K, respectively. $Sn_4P_3$ (**3**)[38,39] at 823 and 873 K, AuSn (**4**)[40,41] at 923 K, and **2**[27] in both cases were identified as side products of the reaction. While the amount of side products is relatively small, **1** is grown in large crystals on top of those materials as shown in Figure 1. Tin(IV) iodide, used as a mineralizing agent, and a very small amount of P(red)/P(violet) can be found on the ampule walls after the reaction.

Obviously the tin(IV) iodide (boiling point 629 K at standard conditions)[42] was condensed from the gas phase during the cool down of the samples. We could not find any

(34) Krabbes, G.; Oppermann, H.; Wolf, E. *Z. Anorg. Allg. Chem.* **1975**, *416*, 65−82.
(35) Krabbes, G.; Bieger, W.; Sommer, K.-H.; Söhnel, T. *GMIN, im Programmpaket TRAGMIN zur Gleichgewichtsberechnung*, version 4.01; IFW Dresden, Inst. für Anorganische Chemie TU: Dresden, Germany.
(36) Knacke, O.; Kubaschewski, O.; Hesselmann, K. In *Thermochemical Properties of Inorganic Substances*; Springer: Berlin, 1991.
(37) Barin, I. In *Thermochemical Data of Pure Substances*; VCH: Weinheim, Germany, 1989.
(38) Eckerlin, P.; Kischio, W. *Z. Anorg. Allg. Chem.* **1968**, *363*, 1−9.
(39) Kuz'ma, Yu. B.; Chikhrii, S. I.; Davydov, V. N. *Neorg. Mater.* **1999**, *35*, 17.
(40) Jan, J.-P.; Pearson, W. B.; Kjekshus, A.; Woods, S. B. *Can. J. Phys.* **1963**, *41*, 2252−2266.
(41) Charlton, J. S.; Cordey-Hayes, M.; Harris, I. R. *J. Less-Common Met.* **1970**, *20*, 105−107.
(42) Zhamskaya, N. N.; Titov, V. A.; Titov, A. A.; Kokovin, G. A. *Zh. Fiz. Khim.* **1977**, *51*, 1277.

**Table 2.** Summary of Different Preparation Routes under Low-Pressure and High-Temperature Conditions Tested for the Preparation of Black Phosphorus[a]

| starting materials and starting composition (molar ratio) | temp (K) | products observed |
|---|---|---|
| Au, Sn, red P, $SnI_4$ (1:1:14 :0.045) | 873 | black P, $Au_3SnP_7$, $Sn_4P_3$, $SnI_4$ |
| Au, Sn, red P, $SnI_4$ (1:1:14 :0.045) | 923 | black P, $Au_3SnP_7$, AuSn, $SnI_4$ |
| P(red), $SnI_4$ (14:0.045) | 873 | Hittorf's phosphorus, $SnI_4$ |
| P(red), $SnI_4$, black P crystals (14:0.045:0.045) | 873 | Hittorf's phosphorus, $SnI_4$ |
| Au, P(red), $SnI_4$ (1:14:0.045) | 873 | $Au_2P_3$, white P, red P |
| Au, P(red) (1:14) | 873 | $Au_2P_3$, red P |
| Sn, P(red), $SnI_4$ (1:14:0.045) | 873 | $Sn_4P_3$, Hittorf's phosphorus |
| $Au_2P_3$, P(red) (1:14) | 873 | no reaction, Hittorf's phosphorus |
| $Au_2P_3$, P(red), $SnI_4$ (1:14:0.045) | 873 | no reaction, Hittorf's phosphorus |
| $Au_3SnP_7$, P(red), $SnI_4$ (1:14:0.045) | 873 | no reaction, Hittorf's phosphorus |
| $Ag_3SnP_7$, P(red), $SnI_4$ (1:14:0.045) | 873 | no reaction, Hittorf's phosphorus |
| $Ag_3SnP_7$, P(red) (1:14) | 873 | no reaction, Hittorf's phosphorus |
| $Au_3SnP_7$ | 1073 | $Au_2P_3$, AuSn, P(black) |

[a] Results from phase analytical investigations are given. The term "no reaction" is used if the starting materials remained unchanged during the process.

products pointing toward a reaction or reduction of the tin(IV) iodide in reasonable amounts. Also the expected comproportionation of $SnI_4$ and Sn to $SnI_2$, usually found with significant reaction rates in a temperature range from 523 to 633 K,[43,44] was not observed, probably because Sn and $SnI_4$ were not in direct contact with each other in the liquid phase at that temperature. $SnI_4$ can be evaporated from the bulk residue in reasonable amounts at 453 K before the comproportionation temperature is reached.[45] Decomposition or a chemical reaction of tin(IV) iodide with the starting materials should lead to phases like $Au_7P_{10}I$, $PI_3$, $P_2I_4$, or $AuI_3$ which have been prepared by chemical transport with iodine or directly from the elements using the present reaction conditions.[46,47] We found no hints for the formation of any of those compounds by X-ray or EDX phase analytical investigations.

To optimize the preparation conditions of this surprisingly easy and effective method for the production of **1**, we have performed different preparation strategies. A careful EDX and powder diffraction phase analysis was done after each preparation procedure to verify the products formed. When $SnI_4$ was used as a starting material, a total amount of 10 mg was added to the mixtures. The total mass of all samples were approximately 0.3 g with a 14 times excess in atomic percent of red phosphorus in relation to gold or tin added. Phase analytical results are summarized in Table 2.

The preparation or, better, the transformation from red to black phosphorus at the present conditions is only successful if **2** is formed during the reaction. All attempts to transform the phosphorus by addition of only one of the two metals forming **2** or $SnI_4$ alone failed completely. Also the transformation did not occur if **2** is prepared in advance to the P(red)/P(black) transformation by a common solid-state reaction at moderate temperatures. It can be concluded that in situ prepared **2** plays a key role in the transformation process of red to black phosphorus. Thermal decomposition of **2** at 1073 K in the evacuated silica ampules led to the formation of $Au_2P_3$, **4**, and **1**. The occurrence of **1** was substantiated by X-ray powder-phase analysis. Figure 1 (picture 2) shows **1** found after the thermal treatment of **2** at 1073 K for 4 h and cooling to room temperature at a rate of 150 K $h^{-1}$.

**Table 3.** Crystallographic Data of **1**[a]

| | |
|---|---|
| molar mass (g $mol^{-1}$) | 31 |
| space group | *Cmce* (No. 64) |
| cryst syst | orthorhombic |
| lattice params (Å) | $a = 3.3164(5)$, $b = 10.484(3)$, $c = 4.3793(5)$[b] |
| vol (Å$^3$) | 152.26(5) |
| Z | 8 |
| $\rho_{(X-ray)}$ (g $cm^{-3}$) | 2.70 |
| *hkl* range | $-4 \le h \le 4$, $-15 \le k \le 14$, $-6 \le l \le 6$ |
| cryst color | black |
| cryst size (mm) | 0.26 × 0.20 × 0.01 |
| $\theta$ range (deg) | 9.1−30.2 |
| abs correction | numerical correction after optimization of crystal shape from symmetry equivalent reflns[33] |
| $\mu$(X-ray) ($mm^{-1}$) | 2.15 |
| | 0.598/0.926 |
| reflns total (completeness) | 688 (0.955) |
| independent reflns | 127 |
| reflns $I > 3\sigma I$ | 122 |
| params | 8 |
| $R_{int}$ | 0.0628 |
| $R1$ ($I > 3\sigma I$) | 0.0177 |
| w$R2$ ($I > 3\sigma I$) | 0.0454 |
| $R1$ (all) | 0.0187 |
| *wR2* (all) | 0.0464 |
| res. electron density (e Å$^{-3}$) | +0.13/−0.15 |
| GOF | 1.16 |

[a] Further details on the crystal structure investigations can be obtained from the Fachinformationzentrum Karlsruhe, 76344 Eggenstein-Leopoldshafen, Germany (Fax: (49) 7247−808-666. E-mail: crysdata@fiz-karlsruhe.de) with depository number CSD 417180. [b] Lattice parameters from X-ray powder diffraction.

**Crystal Structure Redetermination and Phase Analytical Results of Black Phosphorus.** The quality and purity of **1** was checked by different methods. A single-crystal structure determination (Table 3), and X-ray powder diffraction phase analysis proved the excellent crystal quality. The structure was refined to final R values of R1 = 0.0177 and wR2 = 0.0454 for all 127 reflections and 8 parameters.[48]

(43) Reinders, W.; de Lange, S. *Z. Anorg. Allg. Chem.* **1913**, *79*, 230−238.
(44) Bontchev, T.; Christov, D.; Manuschev, B. *Z. Anorg. Allg. Chem.* **1970**, *379*, 95−105.
(45) Moeller, T.; Edwards, D. C. *Inorg. Synth.* **1953**, *4*, 119.
(46) Binnewies, M. *Z. Naturforsch* **1978**, *33b*, 570−571.
(47) Jeitschko, W.; Möller, M. H. *Acta Crystallogr., Sect. B* **1979**, *35*, 573−579.
(48) Petricek, V.; Dusek, M.; Palatinus, L. *Jana2000, The Crystallographic Computing System*; Institute of Physics: Prague, Czech Republic, 2000.

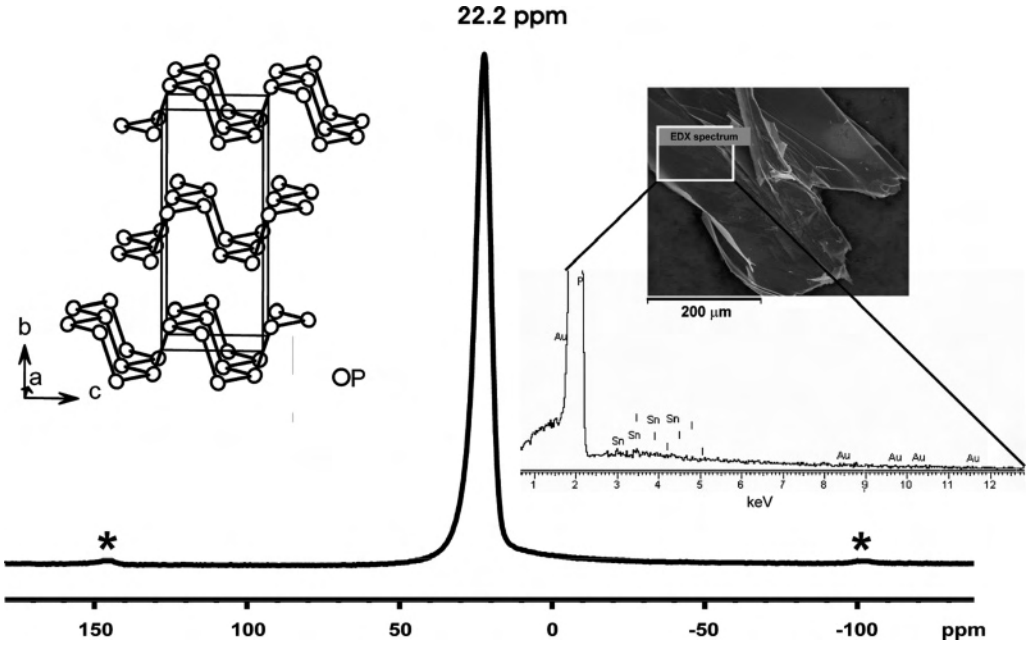


**Figure 2.** Crystal structure (P at 0, 0.10162(2), 0.08068(5); $U_{iso} = 0.0120(2)$ Å$^2$), displacement parameters at 90% probability, $^{31}$P MAS NMR spectrum, and area EDX scan of **1**. The expected positions of the Au, Sn, and I peaks are marked in the EDX plot.

**Table 4.** Comparison of Lattice Parameters, Bond Lengths and Angles of (**1**)

| *a* (Å) | *b* (Å) | *c* (Å) | *d*(P−P) (Å) | ∠(P−P−P) (deg) | density (g cm$^{-3}$) | ref |
|---|---|---|---|---|---|---|
| 3.31 | 10.50 | 4.38 | 2.28 | | 2.69 | 5[a] |
| 3.31 | 10.50 | 4.38 | | | 2.69 | 49[a] |
| 3.3136(5) | 10.478(1) | 4.3763(5) | 2.224 | 96.5 | | 14 |
| | | | 2.244 | 101.9 | | |
| 3.3164(5) | 10.484(1) | 4.3793(5) | 2.2244(2) | 96.38(1) | 2.701 | this work |
| | | | 2.2449(3) | 102.11(1) | | |

[a] Data transformed to *Cmce* for better comparison.

We could not find any hint for a severe stacking disorder, leading to a bad crystal quality as observed by other preparation methods.[14,18]

Very good agreement for all crystallographic data was achieved. To verify the purity of **1**, we performed EDX analyses and $^{31}$P NMR spectroscopy. We could not detect any of the elements other than the phosphorus used in the preparation process. A representative EDX plot and the $^{31}$P MAS NMR spectroscopic data are given in Figure 2. The NMR experiments showed only one sharp signal at 22.2 ppm. Additional signals of red phosphorus or other phosphorus containing materials were not detected.

Single crystals of **2** could be isolated, and semiquantitative EDX measurements revealed a composition of Au (25.9 at. %)/Sn (9.6 at. %)/P (64.5 at. %) very close to the ideal composition of Au (27.3 at. %)/Sn (9.1 at. %)/P (63.6 at. %). A single-crystal structure determination substantiated the formation of [$Au_3Sn$] heteroclusters embedded in $\left[{}^1_\infty P_7\right]$ polymer units. X-ray powder-phase analysis and single-crystal structure analysis proved the formation of monoclinic **2** with lattice parameters of $a = 6.219(2)$ Å, $b = 10.836(2)$ Å, $c = 6.318(2)$ Å, $\beta = 108.65(2)°$, $V = 403.4(2)$ Å$^3$, and space group $P2_1/m$ (No. 11). Figure 3 illustrates the crystal structure of **2**. A detailed description of the crystal structure is given elsewhere, and additional information can be obtained from FIZ Karlsruhe, Germany, depository number CSD 416407.[27]

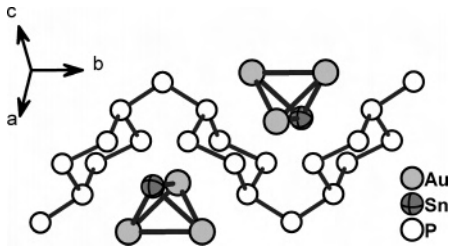


**Figure 3.** Section of the crystal structure of $Au_3SnP_7$ (**2**).[27]

**Mechanistic Aspects.** To get a deeper insight in the present reaction mechanism, we tried to analyze the nature of the reaction to determine if the preparation is either thermodynamically or kinetically controlled. We therefore performed thermodynamic calculations of solid-state and gas-phase equilibria in the system Au/Sn/P/(I). The general procedure of the determination of thermodynamic standard data like $\Delta H^\circ_B$ and $S°$ is given in the experimental section. All calculations are based on known and optimized thermodynamic data of the elements and the condensed phases $Au_3SnP_{7(s)}$, $Au_2P_{3(s)}$, $AuSn_{(s)}$, $AuSn_{2(s)}$, $AuSn_{4(s)}$, $Sn_4P_{3(s)}$, and $Sn_3P_{4(s)}$. For the calculation of the gas-phase equilibrium, we have included the species $Au_{(g)}$, $Sn_{(g)}$, $P_{4(g)}$, $P_{2(g)}$, $P_{(g)}$, and $SnI_{4(g)}$ and, because of a possible but not observed decomposition or comproportionation (see section preparative aspects) of the reaction promoter $SnI_4$, the species $PI_{3(g)}$, $I_{2(g)}$, $I_{(g)}$, and $SnI_{2(g)}$. Our general purpose is to explain the coexistence of $Au_3SnP_{7(s)}$, $AuSn_{(s)}$, and $Sn_4P_{3(s)}$ found experimentally. Figure 4 illustrates the phase fields of the system Au/Sn/P/(I).

The quality of the estimated and optimized thermodynamic standard values (Table 1) used for these calculations can be

(49) Thiel, H. *Ann. Phys.* **1956**, *17*, 122−125.

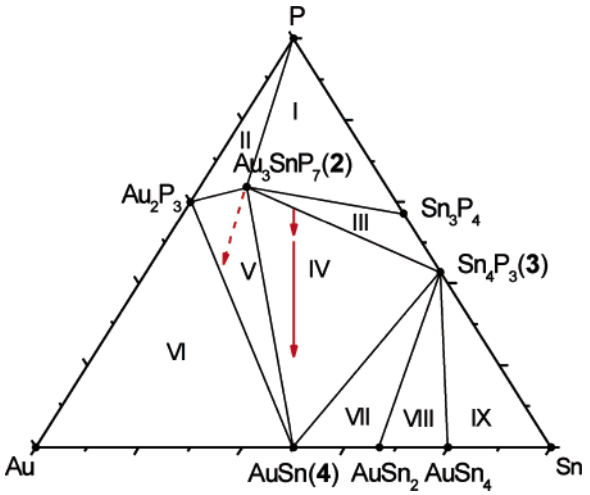


**Figure 4.** Ternary system Au/Sn/P. Gas-phase equilibrium at 873 K are calculated with the program TRAGMIN based on values given in Table 4 and the phase relation within this phase diagram.[35] Compounds **2** and **3** within phase field IV were observed as crystalline materials during the preparation process of **1** at 873 K.

determined from the equilibrium pressure derived from the phase field I in Figure 4 ($P/Au_3SnP_7/Sn_3P_4$). One should get the equilibrium pressure of the compound showing the highest partial pressure in this field, that is, P(red) (Figure 5). The tabulated values found in the literature were exactly reproduced by the present calculations.[36]

The calculation of solid-state−gas-phase equilibrium of different phase fields showed that $P_{4(g)}$ is the dominate gas-phase species in all cases. For phase field IV ($Au_3SnP_7/Sn_4P_3$/AuSn), Figure 4, which was found to be the important one for the formation of **1**, this is also true. Compared with phase field I, the $P_{4(g)}$ equilibrium pressure is reduced by approximately 2 orders of magnitude because of the stabilization of the ternary phase. If a tin-rich bulk phase is present, the decomposition should take place toward **3** and **4**. The composition of the resulting bulk phase is dependent on the temperature and gas volume present for the realization of equilibrium conditions. One can predict that, at low temperatures and small volumes, $\mathbf{3}_{(s)}$ will be the main phase and, at higher temperatures and larger volumes, there will be predominant formation of $\mathbf{4}_{(s)}$. This prediction was confirmed experimentally, as can be seen in Table 2.

To get a deeper insight into possible gas-phase reactions, the distribution and development of partial pressures needs to be discussed. Because of the relatively low temperature of $T \leq 923$ K, the dissociation of $P_{4(g)}$ to $P_{2(g)}$ does not significantly contribute to the gas-phase composition. The partial pressure of $SnI_{2(g)}$, the second-highest one according the theoretical calculations, is dependent on the amount of iodine in the system. At low-temperature conditions, small volumes, and large iodine contents, $SnI_{2(s,l)}$ condenses with the bulk, and one observes the saturation pressure of the $SnI_2$ evaporation (see Figure 5). Further iodide-containing gas-phase species like the starting material $SnI_4$ or possible reaction products like $PI_3$ have no significant contributions (partial pressures $p(i) < 10^{-5}$ bar) toward the bulk or gas-phase transport reactions. It has to be stated at this stage that none of the iodide-containing phases except the starting

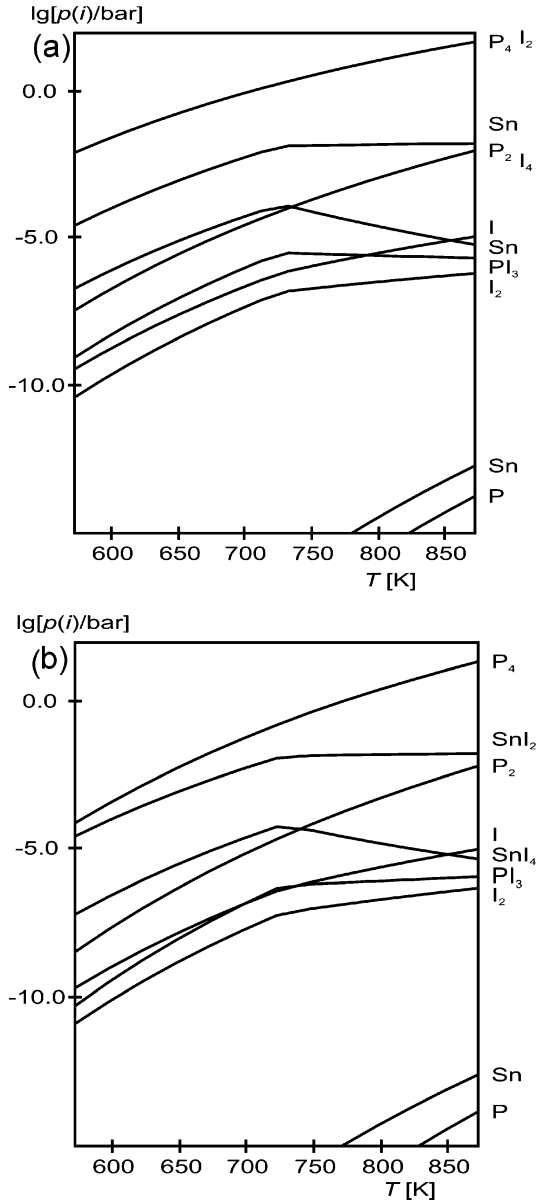


**Figure 5.** (a) Partial pressures on top of solid material of phase field I ($P/Au_3SnP_7/Sn_3P_4$) and (b) of phase field IV ($Au_3SnP_7/Sn_4P_3$/AuSn) according to Figure 4.

material $SnI_4$ were observed by careful EDX or X-ray powder-phase analysis. The observation that **1** grows on top of the bulk material (see Figure 1) forced us to examine if at least a short-range transport of material might occur in the present system. Because no relevant gold species are present in the gas phase, a vapor transport of **2** $Au_3SnP_{7(s)}$ is not possible. In general, a formation of tin phosphide is possible dependent on the iodine partial pressure. According to the gas-phase reaction

$$Sn_3P_{4(s)} + 3I_{2(g)} \rightleftharpoons 3SnI_{2(g)} + P_{4(g)}$$

$$\Delta G_R^\circ(1000) = -280 \text{ kJ mol}^{-1}$$

tin phosphide can be formed close to the bulk residue by a a mineralization mechanism. The partial pressures of $I_{(g)}$ and $I_{2(g)}$ are reduced by 5 orders of magnitude compared with that of $SnI_{2(g)}$ because of the equilibrium conditions in the

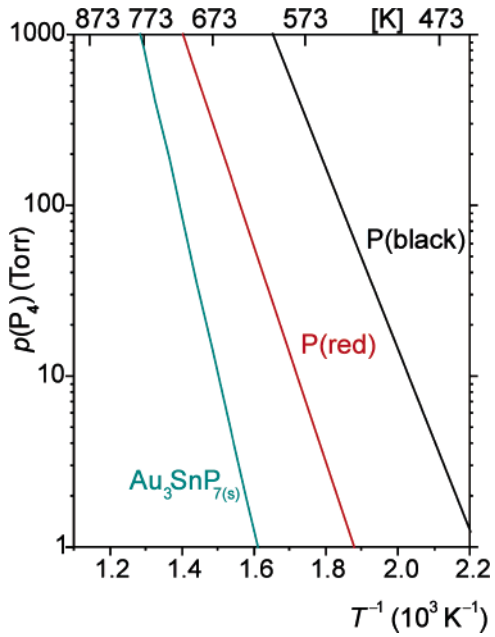


**Figure 6.** Phase barogram of the Au/Sn/P system (873 K), calculated from thermodynamic data according to Table 4 using the program TRAGMIN.[35] $P_4$ was used as the dominating gas-phase species.

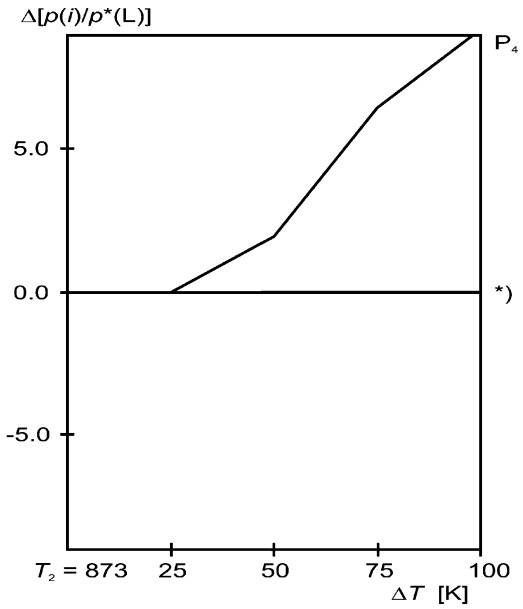


**Figure 7.** Transport efficiencies of all gas-phase species in the phase field IV ($Au_3SnP_7/Sn_4P_3$/AuSn, Figure 4) calculated using the program TRAGMIN.[35] (*) Transport efficiency = 0 for $SnI_2$(g), $P_2$(g), I(g), $I_2$(g), $SnI_4$(g), and $PI_3$(g).

reaction. The equilibrium of this formal transport reaction is located on the far right-hand side because of the stability of $SnI_{2(g)}$ and does not really satisfy the equilibrium conditions ($-80 < \Delta G_R^\circ < +80$ kJ mol$^{-1}$) necessary for chemical transport. Only very small transport rates ($m/t < 0.1$ mg h$^{-1}$) can be expected. We found no experimental hints for a formation of $SnI_2$ or for chemical transport of tin phosphides during our preparations. The total pressures of the solid phases are given in Figure 6.

According to Figure 6, **1** is the thermodynamically instable phosphorus modification compared with P(red) within the temperature range of 473−873 K. A thermodynamically controlled condensation of **1** from the gas phase is therefore not possible. In the phase barogram, a given phosphorus partial pressure has to cross the equilibrium line of P(red) within a time and space averaged temperature gradient before condensation. This is not the case, as one can see in Figure 6.

For the main gas-phase species, that is, $P_4$(g), it must be taken into account that the partial pressure can be changed by a decomposition of $\mathbf{2}_{(s)}$. A partial decomposition of **2** will lead to a certain contribution to the $P_{4(g)}$ partial pressure in relation to a pure evaporation of $P_4$ from P(red). Higher-temperature, as well as lower-pressure, conditions have to be considered. Those variations in synthesis conditions might be responsible for a kinetically, rather than thermodynamically, controlled formation of **1** from P(red).

To substantiate the experimental observation that no short-range transport occurs, a calculation of the transport efficiency of the gas-phase species ($\Delta p(i)/p^*(L)$) was performed. Figure 7 clearly summarizes all relevant transport species in the Au/Sn/P(I) system.[50]

Gold and tin phases are not transport relevant ($\Delta p(i)/p^*(L) = 0$). A negative transport efficiency ($\Delta p(i)/p^*(L) < 0$) cannot be observed for any phases in the system, and therefore, a transport can only be done without a transport reagent. The observed condensation of small amounts of phosphorus at the ampule walls is the result of the evaporation or decomposition sublimation from the complex bulk residue. The increase of the positive $P_{4(g)}$ transport gradient at $\Delta T > 30$ K is consistent with the partial pressure difference of $\mathbf{2}_{(s)}$ and P(red) at equilibrium conditions. At temperature differences smaller than 30 K, the conditions for a condensation of $P_{4(s)}$ are not satisfied and $P_{4(g)}$ remains in the gas phase. This theoretical finding is consistent with the experimental observation that condensation only of a small amount of phosphorus to the ampule walls took place after cooling to room temperature. The condensation of **1** should take place in a time- and space-dependent temperature gradient of about 150 K (Figure 5). According to a thermodynamically controlled condensation of **1**, the partial pressure would be reduced by the condensation of P(red).

A thermodynamically motivated formation of **1** cannot be responsible in our case, and a more kinetically controlled mechanism must be considered for the preparation of **1** at low-pressure and high-temperature conditions.

**Kinetically Motivated Aspects in the Preparation of P(black).** A comparison of the crystal structures of **1** and **2** points toward some interesting topological structural features of the phosphorus substructures in both materials. Looking along the (100) plane in **1** and along the (010) plane in **2**, one can find an arrangement of six-membered P ring fragments with very similar distances between each other. Figure 8 represents the phosphorus substructures of both materials orientated toward each other in such a way that those features become obvious.

(50) Oppermann, H.; Reichelt, W.; Krabbes, G.; Wolf, E. *Kristall Tech.* **1977**, *12*, 919.

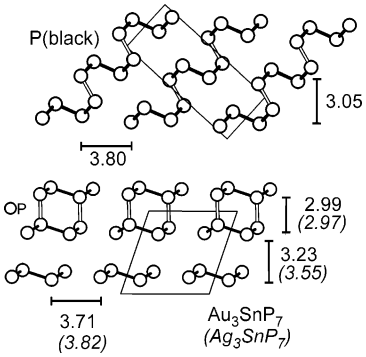


**Figure 8.** Sections of the P substructures of **1** (view on (100), top part), **2**, and $Au_3SnP_7$ (view on (010), bottom part). Comparable P ring fragments are highlighted by solid black lines. Distances (in Å) of $Ag_3SnP_7$ are given in italics.[30]

Focusing on the translation periods of the six-membered $P_6$ ring fragments, one can observe almost equal distances for the P ring itself and the intramolecular distances between the fragments. The tilt of the neighboring $P_6$ rings relative to each other might be tolerable for such a mechanism, while the increase in the $P_6$ ring distance (3.23−3.55 Å, see Figure 8) going from **2** to $Ag_3SnP_7$[30] led to a failure of a P(red)/P(black) transformation. From the interpretation of the results from the different preparation routes performed, an epitactic growth of black phosphorus on **2** is at least possible.

Further experiments such as transmission electron microscopy at the phase boundary between the two materials are planned to substantiate this assumption. Also temperature-dependent X-ray powder diffraction at elevated temperatures may lead to a better understanding of the formation of crystalline solid phases during the preparation process.

## Conclusion

The preparation of **1** can be easily performed using equimolar amounts of gold and tin, an excess of P(red), and catalytic amounts of tin(IV) iodide at low-pressure conditions in quartz glass ampules. This preparational route represents an elementary discovery in the chemistry of phosphorus and simplifies the production process of **1** drastically. High-quality crystals in reasonable sizes and amounts can be prepared in a more effective way than using formerly developed methods. The purity, physical properties, and crystal structure of **1** have been redetermined to exclude significant doping with starting material during the preparation process. A thermodynamically motivated formation of **1** was excluded from thermodynamic calculations of solid-state and gas-phase equilibria. No significant transport of material, except the phosphorus transport via $P_{4(g)}$ molecules leading to P(red), could be identified. According to experimental results and based on comparable structural features of **1** and **2**, formed during the preparation process, an epitactic growing mechanism is suggested as one possible kinetically motivated mechanism for the formation of **1**.

**Acknowledgment.** The authors thank Dr. L. Zhang and Prof. Dr. H. Eckert, University of Münster, Germany for the measurement of a $^{31}P$ MAS NMR spectrum. This work is financed by the Deutsche Forschungsgemeinschaft (DFG), grant NI 1095/1-1.

**Supporting Information Available:** CIF file of **1**. This material is available free of charge via the Internet at http://pubs.acs.org.

IC062192Q